A LABORATORY STUDY OF CURRENT EFFICIENCY IN CRYOLITIC MELTS

P.A.Solli*, T.Haarberg*, T.Eggen**, E.Skybakmoen** and Å. Sterten**

* Hydro Aluminium, Technology Centre Årdal, P.O Box 303, N-5870 Øvre Årdal, Norway

** Department of Electrochemistry, Norwegian Institute of Technology, N-7034 Trondheim, Norway

ABSTRACT

Results are presented from a study of the influence of bath composition, temperature, cathodic current density, interpolar distance and bath impurities on the current efficiency with respect to aluminium in a laboratory cell. The current efficiency was determined from the weight gain of the metal pad, in a laboratory cell specifically designed to attain good and reproducible convective conditions, and with a flat aluminium cathode surface which ensures even current density distribution on the aluminium pad surface. The cell is believed to more closely represent conditions in commercial cells than traditional small scale laboratory cells. The results are compared to previously reported results, and a current efficiency model is presented.

INTRODUCTION

The influence of bath and electrolysis variables on the current efficiency (CE) with respect to aluminium in the Hall-Héroult process has been investigated by a great number of workers. Literature reviews have been given by Grjotheim et al[1] and Kvande[2], and there is still some dispute as to the effect of some variables, especially the effect of alumina concentration in the electrolyte. The purpose of the present work has been to carry out an extensive study of the influence of important variables on CE by a procedure and in a laboratory cell which is expected to give mass transport- and current density distribution conditions more representative to conditions in commercial cells, compared to the traditional laboratory cell designs.

Sterten[3] has developed a CE model based on theory of electrochemistry and mass transport. The model has been modified, and unknown parameters determined empirically from the present results. A simplified version of the new model is given in the present paper, whereas details of the model theory are given elsewhere[4,5].

EXPERIMENTAL

Design of the Cell

As shown below CE is highly dependent on the cathodic current density, i.e. the current density on the metal pad surface. The geometry of the metal pad in traditional laboratory cells (hemispherical or spherical shape) may be unfortunate for the current distribution and thus the value of the determined CE. The problem of uneven current distribution due to a rounded shape of the metal pad is eliminated by using a wettable cathode substrate in the cell, which gives a close to flat metal pad. A steel plate is used in the present work, but this leads to dissolution of iron into the liquid aluminium and may cause an aluminium activity lower than 1 and a CE higher than representative for a unit activity aluminium pool. This effect has been calculated to be of negligible importance[4].

Laboratory cells are often characterized by very low bath velocities due to the small scale of the cells. Stagnant layers close to the aluminium pad, and consequently poor reproducibility of determined CEs, may often be the result in such cells. In the present work elimination of this problem has been attempted by designing the anode in such a way as to attain additional convection from the evolution of anode gas bubbles. A cylindrical anode with a vertical hole through the centre, and two horizontal holes in level with the electrolyte surface, as shown in Fig. 1, should in theory cause the anode gas bubbles to escape through the central vertical hole, and the electrolyte to move as indicated by the dotted lines and arrows in Fig. 1. Initial experiments showed that the wear of the corundum side lining of the cell was particularly pronounced close to the horizontal holes in the anode, showing that the electrolyte movement is as desired.

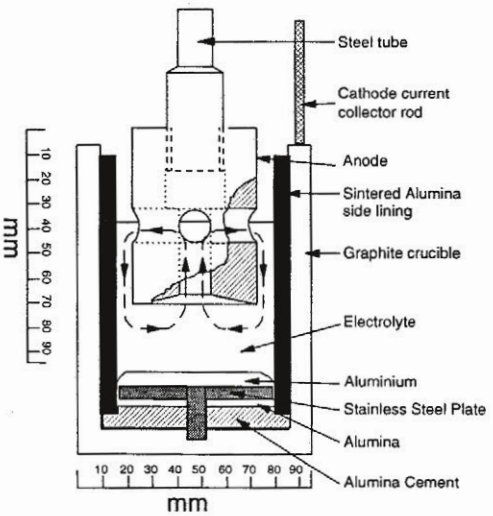

Fig 1: The laboratory cell with bath circulation pattern indicated by dotted lines and arrows.

Procedure

The cell was placed in a vertical tube furnace (argon atmosphere) and positioned in such a way as to avoid temperature gradients in the electrolyte. Alumina was fed to the bath through the central vertical hole of the anode to sustain constant alumina concentration. The CE was determined from the weight gain of the metal (aluminium and steel) after carrying out 4 hour-experiments at constant current. The current was monitored over a standardized ohmic resistance.

G. Bearne et al. (Eds.), *Essential Readings in Light Metals*

The standard electrolysis conditions, or the reference conditions, were as follows,

Cryolite ratio, r : 2.5 (7 wt% AlF_3),

Al_2O_3 : 4 wt%,

CaF_2 : 5 wt%,

T : 980°C,

Cathodic current density : 0.85 A/cm^2,

and interpolar distance 27 mm.

The variables were changed sequentially in order to study the isolated effect of each one of them on current efficiency.

Employment of a sintercorundum (Al_2O_3) side lining inevitably leads to its dissolution, although slow, into the electrolyte. Analysis of the electrolyte at the end of the experiments with presumed (weighed out) concentrations of 4 wt% alumina, revealed alumina contents in the order of 4-6 wt%, i.e. slightly higher than the weighed out amount due to dissolution of the liner.

Investigation of the influence of alumina concentration on the CE was carried out in a pyrolytic boron nitride crucible, where close control of the alumina concentration was attained.

In the experiments with impurity additions, impurities were added according to estimated rates of impurity transfer into the metal and gas phase[4] in order to sustain roughly constant concentrations in the electrolyte.

RESULTS

Cell Performance

Four experiments were carried out for the standard conditions given above. The average CE value was 93.0%, with an absolute standard deviation of only 0.2%. The cathodic overvoltage in the cell was determined as a function of cathodic current density[4], with values in the order of -60 to -70 mV at "normal" current densities. The low overvoltage values and the good CE reproducibility suggest that the cell performs well, with high and reproducible convective conditions in the electrolyte, and values comparable to those found in commercial cells[6]. Fig. 2 shows photographs of two dissected cells from experiments where the interpolar distance was varied. Note the shape of the metal pad and the wear of the corundum lining near the horizontal holes in the anode.

Cathodic Current Density

The cathodic current density was varied between 0.3 and 1.3 A/cm^2 and compared to results obtained by Skybakmoen and Sterten[7] in a virtually identical cell. The results, together with a line representing the CE model, are given in Fig. 3.

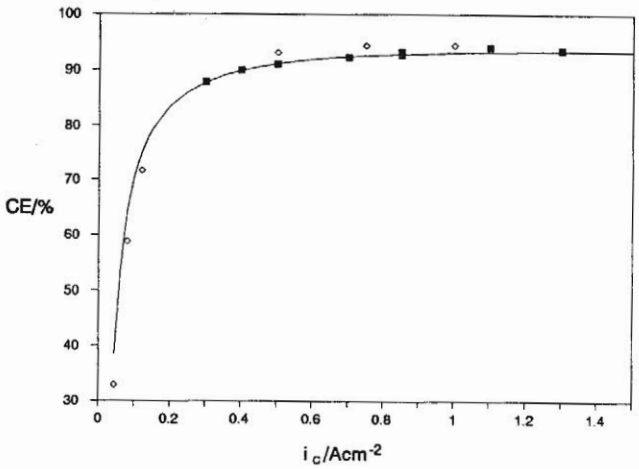

Fig. 3: CE as a function of cathodic current density, i_c. Temperature 980°C, NaF/AlF_3 ratio 2.5, 5 wt% CaF_2 and 4 wt% alumina. Filled squares: present work, diamonds: Skybakmoen and Sterten[7], solid line: CE model.

Most of the results in the literature show an increase in CE with increasing current density[1], although Antipin and Niederkorn[8] found a maximum at 0.8 A/cm^2. Trends similar to the one in Fig. 3 have been obtained by Gjerstad and Richards[9] and Barat et al[10].

Interpolar Distance

The interpolar distance was varied between 6 and 40 mm. The results are shown in Fig. 4, and show that within the experimental uncertainty, the anode-cathode distance does not influence the CE unless at very low anode-cathode distances (below a "critical" value) where direct contact presumably is achieved between the anode gas bubbles and the cathode boundary layer.

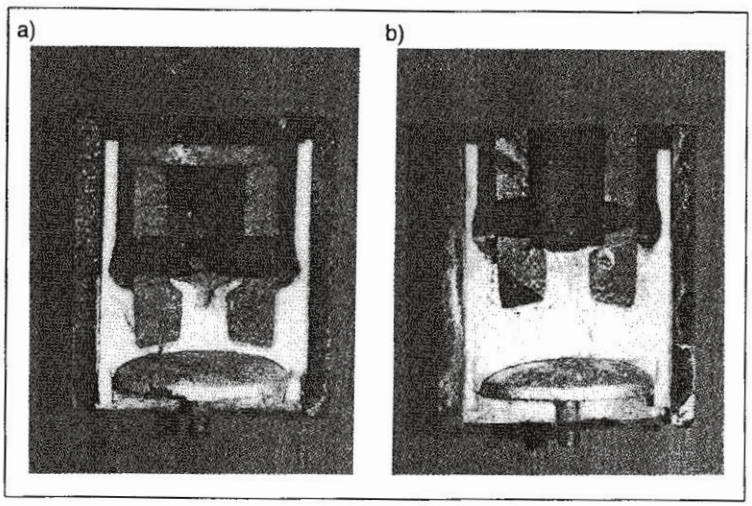

Fig. 2: Photographs of dissected cells with a) interpolar distance 6 mm and b) interpolar distance 27 mm.

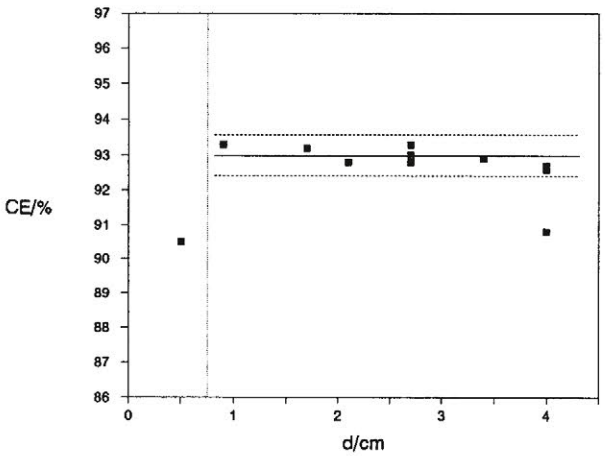

Fig. 4: CE as a function of interpolar distance (d). Temperature 980°C, NaF/AlF_3 ratio 2.5, 5 wt% CaF_2, 4 wt% alumina and cathodic current density 0.85 A/cm^2. The approximate critical anode-cathode distance is indicated by the dotted vertical line.

Reported values of critical interpolar distances in commercial cells are scarce. Rolseth et al.[11] found a value of 25mm (measured from wave tops) while Alcorn et al.[12] reported a value of 40mm. The critical interpolar distance in commercial cells is dependent on metal instability (cell design and ledge geometry) and is greater and less well defined than in our small scale laboratory cell, due to metal pool waves and thicker anode gas bubbles.

NaF/AlF_3 Ratio

CE as a function of NaF molar fraction at constant temperature (980°C) is given in Fig. 5 together with the line representing the CE model. Numeric values are given in Table I. CE as a function of NaF/AlF_3 molar ratio at 980°C roughly follows a straight line, with the slope dCE/dr = -4.2 % per unit ratio.

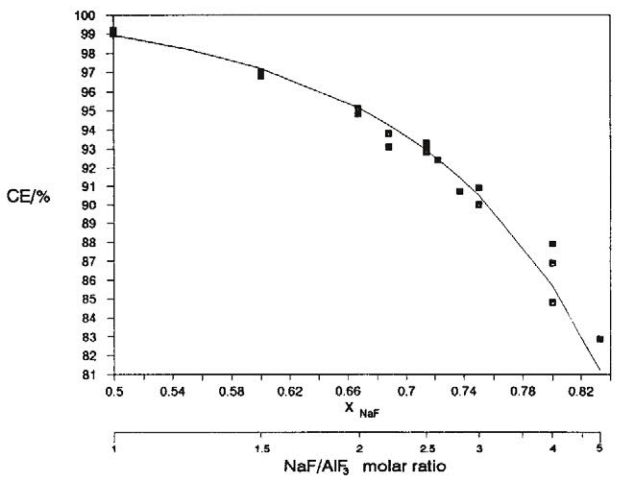

Fig. 5: CE as a function of the NaF molar fraction in the binary NaF-AlF_3 system at 980°C. Points: experimental values. Line: CE model. Cathodic current density 0.85 A/cm^2, 5 wt% CaF_2, 4 wt% alumina, balanced by cryolite and AlF_3.

The effect of ratio (bath acidity) on CE is due to the change of rate of cathodic side reactions (formation of reduced and soluble entities on the metal surface), as predicted by the CE model in terms of the equilibrium activity of sodium metal on unit activity aluminium.

Table I: Numeric values from the study of CE as a function of bath acidity in terms of ratio and wt% excess aluminium fluoride.

NaF/AlF_3 molar ratio (wt% AlF_3)	CE/%	NaF/AlF_3 molar ratio (wt% AlF_3)	CE/%
1.0 (40%)	99.2	2.5	93.3
1.0	99.0	2.5	93.0
1.5 (26%)	97.0	2.6 (5%)	92.4
1.5	96.8	2.8 (3%)	90.7
2.0 (15%)	94.8	3.0 (0%)	90.9
2.0	95.1	3.0	90.0
2.2 (12%)	93.1	4.0	87.9
2.2	93.8	4.0	84.8
2.5 (7%)	93.0	4.0	86.9
2.5	92.8	5.0	82.9

Linear correlations obtained in the present and previous studies are given in Table II. All the results are in fair agreement with the present work, taking uncertainties in determined coefficients into consideration.

Table II: Results from present and previous studies of CE as a function of cryolite molar ratio.

Reference	dCE/dr	Comments
Lewis[13]	-8 ± 2	Constant T, 10 kA test cell, 85-90% CE, determined at r=3 and r=2.6.
Burck and Fern[14]	-8	Constant superheat, 47 kA cells, 85-88%CE, r varied between 2.3 and 2.7.
Berge et al.[15]	-7.8	135 kA prebaked cells, isothermal coefficient at 87-90% CE, r varied between 2.5 and 2.8.
Dewing[16]	 -8.2 -5.9 -4.1 -3.2	Model based on results from Burck and Fern above. Constant superheat. Calculated at 86% CE. Calculated at 90% CE. Calculated at 93% CE. Calculated at 94.5% CE.
Thonstad[17]	-5 ± 2	Laboratory cell, r varied between 2.2 and 3.
Present work	-4.2±0.5 -5.2±1.0 -7.1±1.5	Isothermal conditions, 980°C. Constant superheat, r = 3.0, 90% CE. Constant superheat, r = 2.0-2.5, 96-93% CE.

Temperature

The isolated effect of temperature on CE was studied for three different bath compositions (r = 2.0, 2.5 and 3.0). The results are given in Figs. 6-9, together with lines representing the CE model. The results show that the derivative, dCE/dT, becomes more negative with decreasing efficiency, i.e. with increasing ratio and increasing temperature.

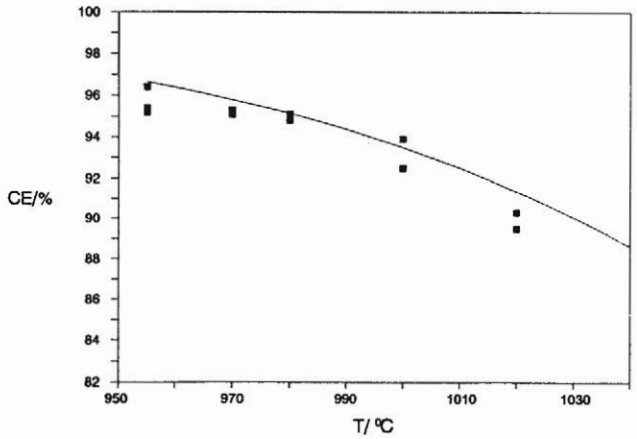

Fig. 6: CE as a function of temperature at r = 2.0. Points: experimental values. Line: CE model. Cathodic current density 0.85 A/cm^2, 5 wt% CaF_2, and 4 wt% alumina.

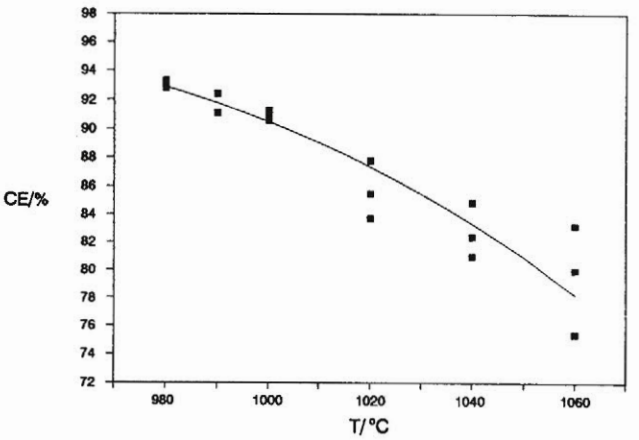

Fig. 7: CE as a function of temperature at r = 2.5. Points: experimental values. Line: CE model. Cathodic current density 0.85 A/cm^2, 5 wt% CaF_2, and 4 wt% alumina.

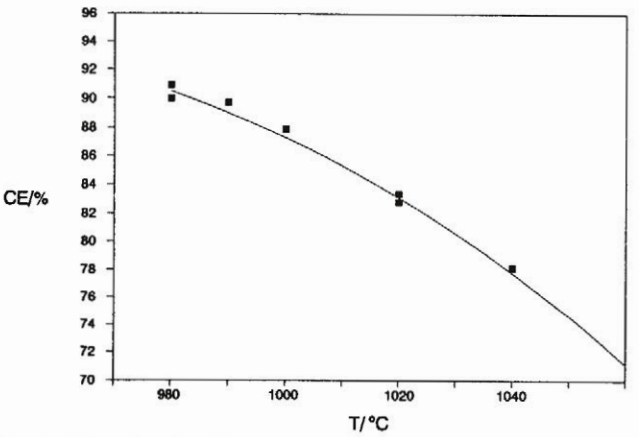

Fig. 8: CE as a function of temperature at r = 3.0. Points: experimental values. Line: CE model. Cathodic current density 0.85 A/cm^2, 5 wt% CaF_2, and 4 wt% alumina.

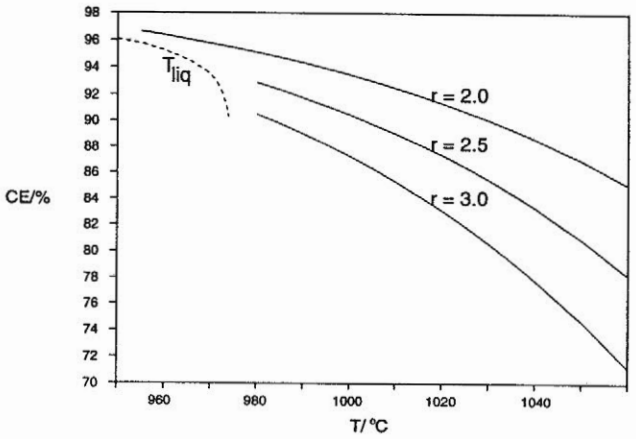

Fig. 9: CE as a function of temperature (T), model lines for cryolite ratios 2.0, 2.5 and 3.0. The liquidus temperature is indicated by the dotted line.

Some previously obtained results from studies of CE as a function of temperature in industrial cells are given in Table III. The results show some discrepancies, and values from studies in industrial cells show slightly more negative dependencies than the present work and most other studies in laboratory cells. The model of Dewing[16] predicts coefficients systematically 40% higher than the present model. The most likely reason is that the model of Dewing includes the effect of temperature on freeze conditions, and thus the effect of an increased aluminium pad surface area and a decrease in cathodic current density with an increase of temperature. The present model only includes the isolated effect on CE due to the influence of temperature on the rate of cathodic side reactions and electronic conduction (transport of reduced and soluble entities).

Table III: Results from studies of temperature on CE in commercial cells and from the present study.

References	dCE/dT (%/K)	Comments
Berge et al.[15]	-0.14	150 kA cells, radioactive tracer dilution.
Poole and Etheridge[18]	min -0.09 max -0.14	Gas analysis, 130 kA cells, 90% CE.
Lillebuen et al.[19]	-0.22	Gas analysis, 175 kA cells.
Alcorn et al.[12]	-0.17 -0.23 -0.16	Horiz. stud Søderberg. Vert. stud Søderberg. Prebaked cell.
Dewing[16]	 -0.09 -0.17 -0.23	Non-linear dependence found in pilot cell. Linearized coefficients at low superheats. CE 97%. CE 93%. CE 90%
Present work	 -0.06 -0.09 -0.12 -0.16	Linearization in given temperature intervals. CE 97%, r=2.0, 960-980°C. CE 95%, r=2.0, 980-1000°C. CE 93%, r=2.5, 980-1000°C. CE 90%, r=3.0, 980-1000°C.

Al_2O_3 Concentration

In the study of CE as a function of alumina concentration a pyrolytic boron nitride crucible (type PBN, SINTEC Keramik GmbH) was used as cell lining material instead of sintered alumina, to attain easy control of the bath alumina concentration. The alumina concentration was varied between 1.2 and 8 wt%, all other variables kept constant, according to the standard conditions above. The results are shown in Fig. 10, and show that within the experimental uncertainty, alumina has roughly no influence on the CE. The constancy of the model line (slope close to zero) reflects that the equilibrium activity of sodium (dissolved metal) is only slightly affected by the alumina concentration. A least squares fit to the experimental data gave a slope dCE/dc_{Al2O3} of 0.0 ± 0.2 %/wt%.

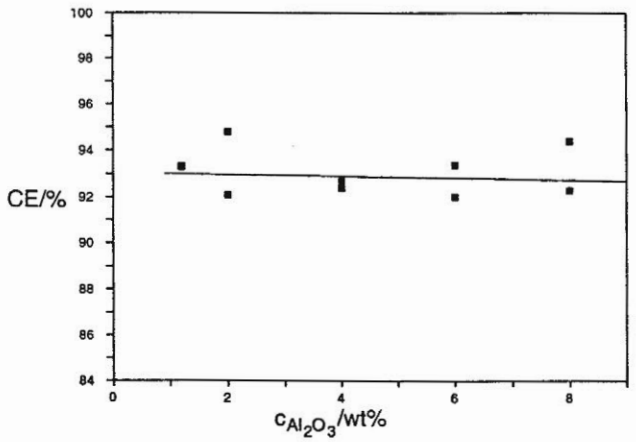

Fig. 10: CE as a function of alumina concentration at constant temperature (980°C). Cathodic current density 0.85 A/cm^2, NaF/AlF_3 molar ratio 2.5, 5 wt% calcium fluoride. Points: experimental values. Line: CE model.

Results from previous investigations show considerable discrepancies as to the isothermal effect of alumina on CE. Both positive and negative correlations have been found, although positive effects are most common. Some results obtained in laboratory cells show a minimum in CE at 4-6 wt% alumina[20,21]. Investigations in industrial cells usually show a considerable isothermal increase of CE with an increase of alumina concentration, but the results obtained from measurements based on analysis of the CO/CO_2 composition of the anode gas may be uncertain due to alumina concentration dependent changes in wetting properties between electrolyte and carbon. An increase in alumina concentration gives an increased wetting of carbon by the electrolyte and a decrease in the contact area between gas bubbles and carbon. This may cause a decrease in the transport rate of CO from the pores in the anode into the anode gas bubbles, and a decrease in the CO content in the collected gas with increasing alumina concentration, as proposed by Leroy et al.[24]. Determination of CE from the CO content in the anode gas may thus give erroneous dependencies due to an alumina concentration dependent error of the Boudouard reaction. Previously reported linearised coefficients are shown in Table IV.

Table IV: Results from the literature of the effect of alumina concentration on CE.

References	$dCE/dc_{alumina}$ (%/wt%)	Comments
Gjerstad and Richards[9]	+1.3	Laboratory cell, CO/CO_2.
Leroy et al.[22]	-2	Industrial cell, mass spectrometry.
Poole and Etheridge[18]	+1.5	Industrial cells, CO/CO_2, non-linear dependence linearized at 3-4wt% alumina.
Lillebuen et al.[23]	+0.05 and +0.57	Two runs, CO/CO_2, Søderberg cells, 85% CE.
Alcorn et al.[12]	+0.2 to 0.6	Industrial cells, CO/CO_2 analysis.
Paulsen et al.[24]	+0.7±0.2	Industrial cells, CO/CO_2 analysis.
Present work	0.0 ± 0.2	Laboratory cell, weight gain of metal.

Calcium Fluoride

The calcium fluoride concentration was varied between 0 and 20 wt%. The results are shown graphically in Fig. 11 and numerically in Table V. The positive effect predicted by the model is due to the effect of calcium fluoride on the thermodynamic solubility of metal, expressed in terms of the equilibrium activity of sodium on unit activity aluminium[4].

It is possible that we were unable to dissolve 4 wt% alumina at 20 wt% calcium fluoride and 980°C. Phase diagram data[1] suggest that we are close to the solubility limit, or that the solubility limit may have been slightly exceeded.

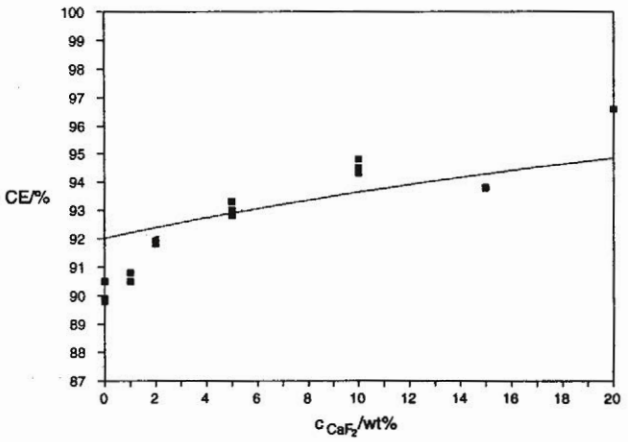

Fig. 11: CE as a function of calcium fluoride concentration. Temperature 980°C, cathodic current density 0.85 A/cm^2, cryolite ratio 2.5 and 4 wt% alumina. Points: experimental values. Line: CE model.

CaF_2 concentrations higher than 8-10 wt% may in industrial cells cause excessive wave formation , with subsequent local events of short circuiting or dispersion of metal. The reasons for this are increasing electrolyte density and high forces of convection in the metal phase, giving increasingly poorer phase seperation between the electrolyte and metal with an increase in calcium fluoride concentration. The effect was apparently unimportant in the laboratory cell, probably due to a more stagnant metal phase.

Previous results from studies in laboratory cells[21,25] show a distinct increase in CE with increasing calcium fluoride concentration, whereas studies in industrial cells[16,24] show no measurable

Table V: Numeric values from the study of CE as a function of calcium fluoride concentration.

c_{CaF2}/wt%	CE/%	c_{CaF2}/wt%	CE/%
0	90.5	5	93.0
0	89.8	5	93.0
0	89.9	5	93.3
1	90.5	10	94.8
1	90.8	10	94.5
2	92.0	10	94.3
2	91.8	15	93.8
2	91.8	20	96.6
5	92.8		

effect. In the industrial cell studies above, the calcium fluoride concentration has been varied only over very narrow ranges of calcium fluoride concentrations, and the expected slight positive effect may in practice be hard to detect.

THE CE MODEL

Model Equations

A detailed description of the underlying theory of the present model is given elsewhere[4,5]. The original model requires a somewhat extensive algorithm and computer programming for calculations of current efficiency. For practical application of the model to commercial cells, it is sufficient to use a simplified version of the model. In the present paper we will only be concerned with the simplified version. Necessary equations (1-6) are given below.

$$CE\ /\ \% = 100\ \frac{i_{Al}}{i_{Al}+i_{loss}} = 100\ \frac{i_c - i_{loss}}{i_c} \qquad (1)$$

$$i_{loss}\ /\ A\ cm^{-2} = F\,k_{mix}\,a_{Na,eq}^{y}\,exp\left[\frac{-yF\eta}{RT}\right] \qquad (2)$$

$$a_{Na,eq} = exp\left[50.633 + \frac{\left(-50498+44000x\right)}{T} - \frac{\left(9.9+35x^2\right)}{x} - \frac{wt\%CaF_2}{19} + \frac{wt\%Al_2O_3}{85}\right] \qquad (3)$$

$$y = 0.33 + 0.07r = 0.33 + 0.07\left(\frac{x}{1-x}\right) \qquad (4)$$

In the above equations i_{Al} is the partial current density of aluminium deposition, i_{loss} the partial current density of all side reactions (responsible for loss of aluminium), and i_c is the total cathodic current density (the sum of the two former partial current densities). The partial current density of side reactions, i_{loss}, is expressed by Eq. 2 in terms of an empirical transport or rate constant, k_{mix}, the equilibrium activity of sodium on unit activity aluminium (corresponding to bulk bath composition), $a_{Na,eq}$, an empirical proportionality constant, y, (determined from the results of CE as a function of NaF/AlF_3 molar ratio) and the cathode diffusion overvoltage, η. The temperature is given by T (K), x denotes the mole fraction of NaF in the binary NaF-AlF_3 system and the NaF/AlF_3 molar ratio is given by r. F denotes Faraday's constant (C/mol) while R is the gas constant (J/Kmol).

The rate constant k_{mix} is partly a mass transport constant and depends on convection. The cathode diffusion overvoltage, η, will to some extent also depend on the convective conditions (diffusion layer thickness). The rate constant k_{mix} was determined from the CE results in the present laboratory cell, and is given by Eq. 5. The experimentally determined cathode overvoltage[4] is approximately given by Eq. 6 (valid for $i_c > 0.05$ A/cm^2).

$$k_{mix}\ /\ mol\ cm^{-2}\ s = exp\left[-0.840 - \frac{15000}{T}\right] \qquad (5)$$

$$\eta\ /\ V = -0.086\,i_c \qquad (6)$$

The model equations above are valid in a slightly more restricted range of current densities and bath acidities than the original model, namely $i_c > 0.05$ A/cm^2 and $r < 3.0$. Eqs. 1-4 are general, while Eqs. 5 and 6 are specific for the convective conditions in the present laboratory cell.

Example of Model Application - Current Density Distribution in A Prebaked Cell

In commercial prebaked aluminium electrolysis cells the surface of the metal pad usually extends 15-30 cm outside the vertical projection of the anode. From simple current distribution theory one should then expect the local cathode current density to decrease towards the side ledge, with a corresponding decrease of the total current efficiency. By applying one of the software computer tools used by Hydro Aluminium in their design strategy (ALCEL3, a 3D finite difference program for calculation of temperature and potential fields), the local cathodic current density was calculated as a function of distance from the side ledge for two markedly different simplified ledge profiles[26]. The effect of horizontal overvoltage gradients on the cathodic current density distribution is not included in the calculations. The profiles with calculated current vectors are given in Fig. 12, and the results of modelled current densities are shown in Fig. 13. The bath composition used in the calculations is 10 wt% AlF_3, 3 wt% alumina and 6 wt% CaF_2, and the temperature is 955°C. The convective conditions are assumed to be similar to those in our laboratory cell, and constant over the whole of the metal pad. Eqs. 1-6 give for the CE as a function of cathodic current density (A/cm^2),

$$CE\ /\ \% = 100\,\frac{i_c - 0.02453\ exp\left(0.3991\,i_c\right)}{i_c} \qquad (7)$$

which is the equation used to calculate the CE as a function of distance from the pot shell, Fig. 14.

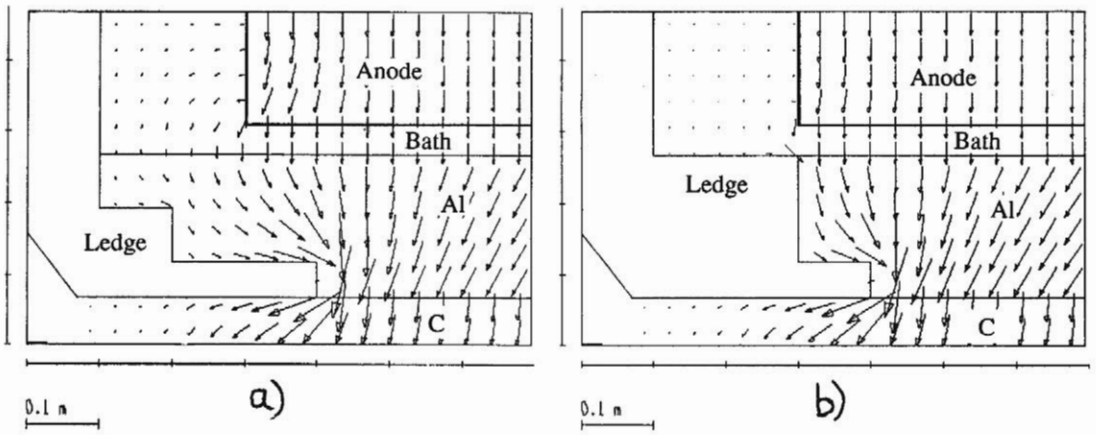

Fig. 12: Cross section through two cells with principally different schematic ledge profiles showing current vectors, a) metal pad extending 20 cm outside the vertical projection of the anode, and b) metal pad not extending beyond the vertical projection of the anode.

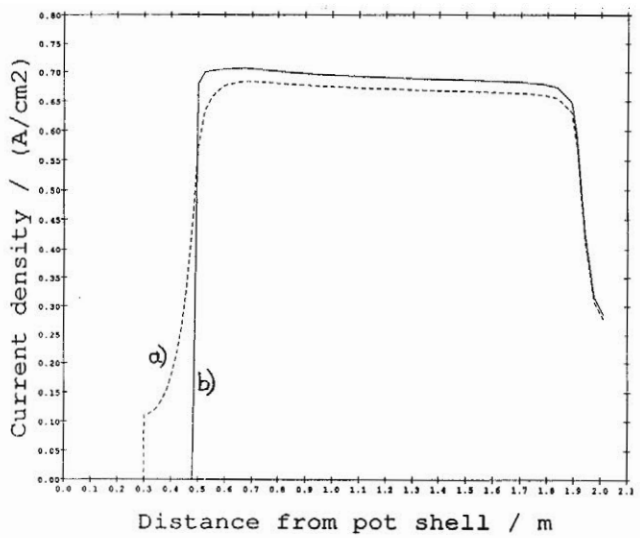

Fig. 13: Local cathodic current density as a function of distance from the pot shell for two different ledge profiles, a) metal pad extending 20 cm outside the vertical projection of the anode, and b) metal pad not extending beyond the vertical projection of the anode.

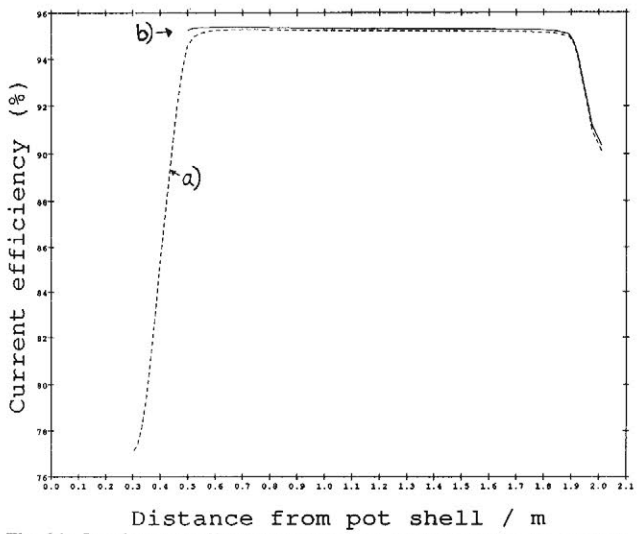

Fig. 14: Local current efficiency as a function of distance from the pot shell, a) metal pad extending 20 cm outside the vertical projection of the anode, and b) metal pad not extending beyond the vertical projection of the anode.

By integrating over the cross sectional area of the metal pad we obtained a total CE of 94.8 for profile a) in Fig. 12, and a CE of 95.2 for profile b), i.e. a 0.4 % reduction of the CE due to a 20 cm extension of the metal pad outside the vertical projection of the anode. By including the additional loss in the end channels, the reduction in CE was 0.6%. Not considered in the present calculations is the possibility of a higher rate of transport in the side channels due to bubble induced convection[27], and mass transport induced by horizontal gradients of surface tension ("Marangoni effect"). These factors may contribute to higher mass transport rates and a greater loss of current efficiency in the channels.

The effect may be considerably greater for Søderberg cells, where the metal pool usually extends 40-70 cm beyond the vertical projection of the anode. This may be an important reason for the low CE values usually observed in Søderberg cells.

BATH IMPURITIES

Experiments were carried out to study the influence of a number of impurity elements (cations) on the CE in the laboratory cell. Added impurity compunds and corresponding cations are shown in Table VI, as well as the investigated range of cation concentrations. Impurities were added with the alumina feed in order to sustain roughly constant impurity concentrations. The individual rates of impurity additions were calculated from estimated mass transfer coefficients (Solli[4]).

Magnesium, barium, copper, boron and tin had apparently no effect on the current efficiency. The other species all reduced the current efficiency markedly. Experimental values are shown for the two most important species in industrial cells, iron and phosphorous, in Figs. 15 and 16, together with regression lines. Note the high uncertainty/spread of values for the experiments with additions of phosphorous species. Only the three lowest phosphorous concentrations were included in the least squares fit in Fig. 16. There was no apparent difference in the Faradaic loss between P_2O_5 additions and $Ca_3(PO_4)_2$ additions. The regression lines of all impurities which were found to have a detrimental effect on CE are given in Fig. 17.

Table VI: Added impurity compounds.

Added impurity	Cation	Cation conc. range (wt%)	Added impurity	Cation	Cation conc. range (wt%)
MgF_2	Mg^{2+}	0-0.05	TiO_2	Ti^{4+}	0-0.10
BaF_2	Ba^{2+}	0-0.24	Ga_2O_3	Ga^{3+}	0-0.15
ZnO	Zn^{2+}	0-0.11	Fe_2O_3	Fe^{3+}	0-0.12
P_2O_5	P^{5+}	0-0.06	CuO	Cu^{2+}	0-0.13
$Ca_3(PO_4)_2$	P^{5+}	0-0.06	B_2O_3	B^{3+}	0-0.02
SiO_2	Si^{4+}	0-0.06	SnO_2	Sn^{4+}	0-0.25
V_2O_5	V^{5+}	0-0.12			

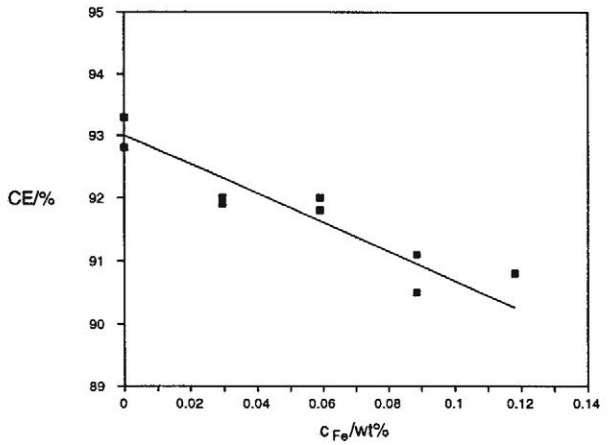

Fig. 15: CE as a function of the total electrolyte concentration of iron cations. Regression line: CE = (93.0±0.5) - (23.2±3.8)c_{Fe}.

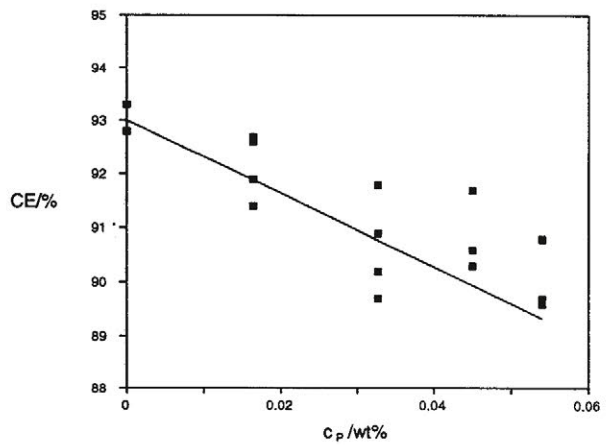

Fig. 16: CE as a function of the total electrolyte concentration of phosphorous cations. Regression line: CE = (93.0±0.5) - (67.8±18.4)c_P.

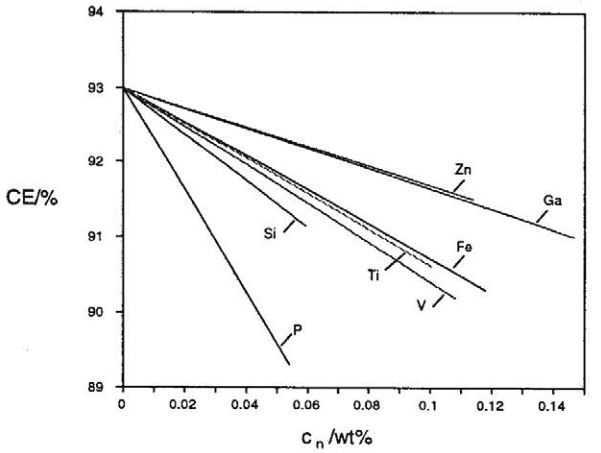

Fig. 17: CE as a function of the total electrolyte concentration of impurity cations (wt%), given as regression lines.

Based on the results (regression lines) and a theoretical model for the reduction of CE due to the participation of impurity species in cyclic redox reactions, the following model was derived for the current efficiency,

$$CE\ /\ \% = CE_{max} - \frac{100}{i_c}\left(0.197c_{Fe} + 0.576c_P + 0.266c_{Si} + 0.244c_V + 0.144c_{Zn} + 0.206c_{Ti} + 0.117c_{Ga}\right) \quad (8)$$

where CE_{max} is the current efficiency with roughly no impurities present in the electrolyte, i_c is the cathodic current density (Acm^{-2}) and c the concentration of impurity species in the electrolyte. The change in CE (ΔCE) can be calculated for a known change of impurity concentration (Δc) by application of Eq. 9.

$$\Delta CE\ /\ \% = -\frac{100}{i_c}\left(0.197\Delta c_{Fe} + 0.576\Delta c_P + 0.266\Delta c_{Si} + 0.244\Delta c_V + 0.144\Delta c_{Zn} + 0.206\Delta c_{Ti} + 0.117\Delta c_{Ga}\right) \quad (9)$$

References

1. Grjotheim,K., Krohn,C., Malinovsky,M., Matiasovsky,K. and Thonstad,J., "Aluminium Electrolysis. Fundamentals of the Hall-Héroult Process", 2nd. edn., Aluminium-Verlag, Dusseldorf (1982).
2. Kvande,H., Light Metals, ed. P.G.Campbell, Proc. of 118th TMS Annual Meeting, Las Vegas (1989), p. 261.
3. Sterten,Å., *J. Appl. Electrochem.* **18**, 473 (1988).
4. Solli,P.A., "Current Efficiency in Aluminium Electrolysis Cells", Dr. Ing. Thesis, Norwegian Institute of Technology (NTH), University of Trondheim, Norway (1993).
5. Solli,P.A. and Sterten,Å., to be published.
6. Rolseth,S., Solheim,A., and Thonstad,J., "Proceedings of the International Symposium on Reduction and Casting of Aluminium", ed. C.Bickert, Vol. 6, Proc. of the Metallurgical Society of the Canadian Inst. of Mining and Metallurgy, Pergamon Press, Montreal (1988).

7. Skybakmoen,E. and Sterten,Å., Internal Report, Electrolysis Group, SINTEF Metallurgy, Trondheim, Norway (1989).
8. Antipin,L.N. and Niederkorn,I., *J. Appl. Chem. USSR* **29**, 577 (1956).
9. Gjerstad,S. and Richards,N.E., *J. Electrochem. Soc.* **113**, 68 (1966).
10. Barat,P., Brault,T. and Saget,J.P., Light Metals, Vol. 1, ed. H.Forberg, Proc. of Sessions 104th AIME Annual Meeting, Dallas (1975), p.37.
11. Rolseth,S., Muftuoglu,T., Solheim,A. and Thonstad,J., Light Metals, ed. R.E.Miller, proc. of 115th TMS Annual Meeting, New Orleans (1986), p.517.
12. Alcorn,T.R., McMinn,C.J., Tabereaux,A.T., Light Metals, ed. L.G.Boxall, 117th TMS Annual Meeting, Phoenix, Arizona (1988), p.683.
13. Lewis,R.A., *J. Metals* **19**, 30 (1967).
14. Burck,J.W. and Fern,D., Light Metals, ed. T.G.Edgeworth, Proc. of Symposia 100th AIME Annual Meeting, New York (1971), p.123.
15. Berge,B., Grjotheim,K., Krohn,C., Næumann,R. and Tørklep,K., Light Metals, ed. S.R.Leavitt, Proc. of Sessions 105th. AIME Annual Meeting, Las Vegas (1976), p.23.
16. Dewing,E.W., *Metall. Trans. B* **22B**, 177 (1991).
17. Thonstad,J., *Can. J. Chem.* **43**, 3429 (1965).
18. Poole,R.T. and Etheridge,C., Light Metals, ed. K.B.Higbie, Proc. of 106th Annual TMS Meeting, Atlanta (1977), p. 163.
19. Lillebuen,B., Mellerud,T., Wallevik,O., Huglen,R. and Berge,T., Paper submitted to Light Metals, Proc. of 114th TMS Annual Meeting,New Orleans (1986).
20. Grjotheim,K., Malinovsky,M., Matiasovsky,K., Silny,A. and Thonstad,J., *Can. Met. Quart.* **11**, 295 (1972).
21. Szeker,C., *Acta Technica Acad. Sci. Hung.* **10**, 19 (1954).
22. Leroy,M.J., Pelekis,T. and Jolas,J.M., Light Metals, ed. R.D.Zabreznik, Proc. of 116th TMS Annual Meeting, Denver (1987), p.291.
23. Lillebuen, B., Ytterdahl,S.A., Huglen,R. and Paulsen,K.A., *Electrochim. Acta* **25**, 131 (1980).
24. Paulsen,K.A., Thonstad,J., Rolseth,S. and Ringstad,T., Light Metals, ed. S.K.Das, Proc. of 122nd TMS Annual Meeting (1993), p.
25. Fellner,P., Grjotheim,K., Matiasovsky,K. and Thonstad,J., *Can. Met. Quart.* **8**, 245 (1969).
26. Haarberg,T., "Current Density Distribution and Magneto-Hydrodynamic Effects in Aluminium Smelters", Modeling in Electrochemistry and Electrochemical Engineering International Workshop, Sept. 1993, Land Brandenburg, Germany (1993).
27. Fraser,K.J., Taylor,M.P. and jenkin,A.M., Light Metals, ed. C.M.Bickert, Proc. of 119th TMS Annual Meeting, Anaheim (1990), p. 221.